

Synthesis and Structure of Two Ionic Copper Indium Selenolate Cluster Complexes $[\text{As}(\text{C}_6\text{H}_5)_4]_2[\text{Cu}_6\text{In}_4(\text{SeC}_6\text{H}_5)_{16}\text{Cl}_4]$ and $[\text{As}(\text{C}_6\text{H}_5)_4][\text{Cu}_7\text{In}_4(\text{SeC}_6\text{H}_5)_{20}]$

Reinhart Ahlrichs,^[a] Nathan R. M. Crawford,^[a] Andreas Eichhöfer,^{*[b]} Dieter Fenske,^[c] Oliver Hampe,^[b] Manfred M. Kappes,^[d] and Jolanta Olkowska-Oetzel^[c]

Keywords: Cluster compounds / Density functional calculations / Mass spectrometry / X-ray diffraction

The reaction of PhSeSiMe_3 , CuCl , InCl_3 , and Ph_4AsCl in CH_2Cl_2 results in crystals of the structurally closely related, ionic clusters $(\text{AsPh}_4)_2[\text{Cu}_6\text{In}_4\text{Cl}_4(\text{SePh})_{16}]$ and $(\text{AsPh}_4)[\text{Cu}_7\text{In}_4(\text{SePh})_{20}]$, with product ratios dependent on the initial PhSeSiMe_3 concentration. Both molecules display a fused four-adamantoid structure related to the solid-state structure of CuInSe_2 . Since the crystallographic analysis for $[\text{Cu}_7\text{In}_4$ -

$(\text{SePh})_{20}]^-$ remained ambiguous with respect to the assignment of one of the copper atoms, we performed a high-resolution mass spectrometric analysis as well as DFT computations to address this problem.

(© Wiley-VCH Verlag GmbH & Co. KGaA, 69451 Weinheim, Germany, 2006)

Introduction

There has been considerable interest in the synthesis and properties of ternary transition metal chalcogenide and chalcogenolate cluster molecules. Examples for different classes of compounds include $[\text{Cu}_6\text{In}_3(\text{SET})_{16}](\text{PPh}_4)_4$,^[1] $[\text{M}^{\text{I}}_6\text{M}^{\text{III}}_8\text{Cl}_4\text{E}_{13}(\text{PPh}_3)_6]$ ($\text{M}^{\text{I}} = \text{Cu}, \text{Ag}$; $\text{M}^{\text{III}} = \text{Ga}, \text{In}$; $\text{E} = \text{S}, \text{Se}$),^[2] $[\text{Cu}_{11}\text{In}_{15}\text{Se}_{16}(\text{SePh})_{24}(\text{PPh}_3)_4]$,^[3] $[\text{Ag}_{26}\text{In}_{18}\text{S}_{36}\text{Cl}_6(\text{dpmp})_{10}(\text{THF})_4][\text{InCl}_4(\text{THF})_2]$,^[4] $[\text{Hg}_{15}\text{Cu}_{20}\text{S}_{25}(\text{P}-n\text{Pr}_3)_{18}]$,^[5,6] $[\text{Cu}_4\text{Nb}_2\text{Se}_6(\text{PMe}_3)_8]$,^[7] $[\text{Ta}_4\text{Cu}_{12}\text{Cl}_8\text{S}_{12}(\text{PMe}_3)_{12}]$,^[8] and $[(\text{N},\text{N},\text{N}',\text{N}'\text{-tmeda})_5\text{Zn}_5\text{Cd}_{11}\text{Se}_{13}(\text{SePh})_6(\text{THF})_2]$.^[9] Interest in these compounds arises for several reasons: (a) investigation of the structural build-up of a certain composition of elements with respect to existing and nonexistent bulk phases, (b) development of precursor compounds for the production of thin films of ternary materials and (c) investigation of the properties of nano-sized species. With respect to (a), it was found that most of the cluster structures formed by elements of group 11–13–16 have, at this stage of growth, no resemblance to the bulk chalcopyrite structure of these materials. On the other hand, stable compounds such as $[\text{Hg}_{15}\text{Cu}_{20}\text{S}_{25}(\text{P}n\text{Pr}_3)_{18}]$ could be formed for compositions of elements that have no stable counterpart

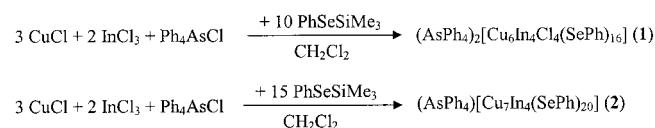
in the bulk phase. Kanatzidis et al. studied the suitability of mixed copper indium chalcogenolates as precursor materials for the photovoltaic materials CuInE_2 ($\text{E} = \text{S}, \text{Se}$).^[1,10] Corrigan et al. observed room-temperature fluorescence for the ternary 12–12'–16 cluster ($12 = \text{Zn}$; $12' = \text{Cd}$; $16 = \text{Se}$), $[(\text{N},\text{N},\text{N}',\text{N}'\text{-tmeda})_5\text{Zn}_5\text{Cd}_{11}\text{Se}_{13}(\text{SePh})_6(\text{THF})_2]$,^[9] while binary cadmium or zinc selenide clusters showed weak luminescence only at temperatures below 50 K. During recent studies, it was found that the investigation of these compounds containing complex mixtures of elements needs a combination of various investigative approaches to reach conclusions with confidence.^[4]

We report herein the synthesis, structural characterization, and theoretical investigation of $[\text{As}(\text{C}_6\text{H}_5)_4]_2[\text{Cu}_6\text{In}_4(\text{SeC}_6\text{H}_5)_{16}\text{Cl}_4]$ and $[\text{As}(\text{C}_6\text{H}_5)_4][\text{Cu}_7\text{In}_4(\text{SeC}_6\text{H}_5)_{20}]$.

Results and Discussion

Synthesis and Structure Determination by X-ray Crystallography

Depending on the amount of PhSeSiMe_3 used, the reaction of CuCl , InCl_3 and Ph_4AsCl in CH_2Cl_2 results in the formation of crystals of either $(\text{AsPh}_4)_2[\text{Cu}_6\text{In}_4\text{Cl}_4(\text{SePh})_{16}]$ (**1**) or $(\text{AsPh}_4)[\text{Cu}_7\text{In}_4(\text{SePh})_{20}]$ (**2**), as outlined in Scheme 1.



Scheme 1.

[a] Institut für Physikalische Chemie, Lehrstuhl für Theoretische Chemie, University of Karlsruhe, Kaiserstr. 12, 76128 Karlsruhe, Germany

[b] Institut für Nanotechnologie, Forschungszentrum Karlsruhe, Germany
Postfach 3640, 76021 Karlsruhe
Fax: +49-7247-82-6368
E-mail: andreas.eichhoefer@int.fzk.de

[c] Institut für Anorganische Chemie, University of Karlsruhe Engesserstraße, Geb. 30.45, 76128 Karlsruhe, Germany

[d] Institut für Physikalische Chemie, University of Karlsruhe, Kaiserstr. 12, 76128 Karlsruhe, Germany

Compound **1** crystallizes in the triclinic space group $P\bar{1}$ (Table 1). The tetrahedrally shaped core of the cluster anion in **1** (Figure 1) is composed of four fused distorted $\{\text{InCu}_3\text{Se}_6\}$ adamantoid cages. In this way, all six copper atoms (Cu1–Cu6) and four μ_3 -SePh[−] ligands (Se1–Se4) build a central adamantoid cage $[\text{Cu}_6(\text{SePh})_4]^{2+}$, which is face-capped by four $[(\mu_2\text{-SePh})_3\text{InCl}]^-$ (In1–In4, Cl1–Cl4) units through μ_2 -SePh ligands (Se5–Se16). All copper and indium atoms display a distorted tetrahedral coordination environment [bond angles: Se–Cu–Se 95.88(6)–124.33(7)°; Se–In–Se 100.35(4)–122.44(4)°; Cl–In–Se 102.44(8)–110.71(8)°]. The Cu– μ_2 -Se bonds {246.16(18) [Cu(2)–Se(6)] to 252.0(2) pm [Cu(1)–Se(8)]} are found to be slightly longer than the corresponding Cu– μ_3 -Se bonds ranging from 239.42(12) (Cu6–Se4) to 245.13(19) pm (Cu3–Se2). The In– μ_2 -SePh bond lengths range from 256.07 (In2–Se14) to 258.30(14) pm (In4–Se9), and the In–Cl bond lengths from 240.5 to 242.8 pm. The so-formed tetrahedral cluster cage is isostructural to known binary and ternary cluster molecules like $[\text{Cd}_{10}(\text{SCH}_2\text{CH}_2\text{OH})_{16}]^{4+}$,^[11] $[\text{M}_{10}\text{E}_4(\text{SPh})_{16}]^{4-}$ (M = Zn, Cd; E = S, Se)^[12,13] $[\text{M}_{10}\text{E}_4(\text{E'Ph})_{12}(\text{PR}_3)_4]$ (M = Zn, Cd, Hg; E, E' = S, Se, Te; R = organic group)^[14–19] and $[\text{In}_{10}\text{Se}_{16}]^{6-}$.^[20]

Table 1. Crystallographic data for $[\text{As}(\text{C}_6\text{H}_5)_4]_2[\text{Cu}_6\text{In}_4(\text{SeC}_6\text{H}_5)_{16}\text{Cl}_4]$ (**1**) and $[\text{As}(\text{C}_6\text{H}_5)_4][\text{Cu}_7\text{In}_4(\text{SeC}_6\text{H}_5)_{20}\text{Cl}_4]$ (**2**).

	1 ·3.5CH ₂ Cl ₂	2 ·4CH ₂ Cl ₂
Molecular mass [g/mol]	4712	4780.3
Crystal system	triclinic	tetragonal
Space group	$P\bar{1}$	$I\bar{4}$
<i>a</i> [Å]	17.660(4)	19.428(3)
<i>b</i> [Å]	18.290(4)	
<i>c</i> [Å]	28.029(6)	21.037(4)
α [°]	88.16(3)	
β [°]	79.96(3)	
γ [°]	82.72(3)	
<i>V</i> [Å ³]	8842(3)	7940(2)
<i>Z</i>	2	2
<i>T</i> [K]	190	190
<i>d</i> _{calc.} [g cm ^{−3}]	1.770	2.097
μ (Mo- <i>K</i> α) [mm ^{−1}]	5.152	6.460
<i>F</i> (000)	4524	4560
2 θ _{max} [°]	50	50
Measured reflexions	54957	20827
Unique reflexions	27884	6891
<i>R</i> _{int}	0.0822	0.0762
Reflexions with <i>I</i> > 2 σ (<i>I</i>)	21130	6136
Refined parameters	1661	406
<i>R</i> ₁ [<i>I</i> > 2 σ (<i>I</i>)] ^[a]	0.0655	0.0394
<i>wR</i> ₂ (all data) ^[b]	0.2299	0.1109
Absolute structure parameter		0.012

[a] $R_1 = \sum ||F_o| - |F_c|| / \sum |F_o|$. [b] $wR_2 = \{\sum [w(F_o^2 - F_c^2)^2] / \sum [w(F_o^2)^2]\}^{1/2}$.

Compound **2** crystallizes in the tetragonal space group $I\bar{4}$ with a crystallographic $\bar{4}$ axis running through As(1) of the Ph_4As^+ cation and Cu(2)/Cu(2') of the cluster anion. The molecular structure of the anion core, $[\text{Cu}_7\text{In}_4(\text{SePh})_{20}]^-$, is, with the exception of two differences, very similar to the structure of **1** (Figure 2). First, the use of an excess of PhSeSiMe_3 leads to an exchange of the terminal chloro ligands with SePh[−] groups. The second, and more remarkable, difference concerns the stoichiometry and

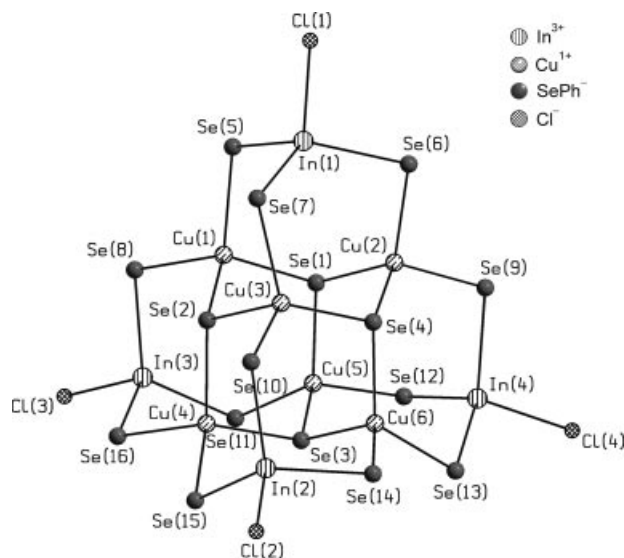


Figure 1. Molecular structure of the cluster anion $[\text{Cu}_6\text{In}_4\text{Cl}_4(\text{SePh})_{16}]^{2-}$ in $(\text{AsPh}_4)_2[\text{Cu}_6\text{In}_4\text{Cl}_4(\text{SePh})_{16}]$ (**1**). C and H atoms are omitted for clarity. Selected bond lengths [pm]: Cu(1)–Se(1) 243.81(17), Cu(1)–Se(2) 244.02(17), Cu(1)–Se(5) 248.25(18), Cu(1)–Se(8) 252.0(2), Cu(2)–Se(1) 242.26(18), Cu(2)–Se(4) 244.24(17), Cu(2)–Se(6) 246.16(18), Cu(2)–Se(9) 249.52(17), Cu(3)–Se(4) 2.4274(17), Cu(3)–Se(2) 245.13(19), Cu(3)–Se(10) 248.88(18), Cu(3)–Se(7) 251.0(2), Cu(4)–Se(3) 242.96(17), Cu(4)–Se(2) 244.83(18), Cu(4)–Se(16) 247.3(2), Cu(4)–Se(15) 247.86(18), Cu(5)–Se(1) 242.72(17), Cu(5)–Se(3) 243.48(17), Cu(5)–Se(11) 246.69(19), Cu(5)–Se(12) 249.57(18), Cu(6)–Se(4) 239.42(18), Cu(6)–Se(3) 241.50(19), Cu(6)–Se(13) 246.40(19), Cu(6)–Se(14) 247.37(19), In(1)–Cl(1) 240.5(3), In(1)–Se(7) 256.57(15), In(1)–Se(5) 257.27(16), In(1)–Se(6) 257.90(14), In(2)–Cl(2) 242.6(3), In(2)–Se(14) 256.07(15), In(2)–Se(15) 256.07(16), In(2)–Se(10) 257.02(16), In(3)–Cl(3) 242.8(3), In(3)–Se(16) 256.14(15), In(3)–Se(11) 256.33(14), In(3)–Se(8) 257.91(15), In(4)–Cl(4) 241.3(3), In(4)–Se(13) 256.16(15), In(4)–Se(12) 257.20(16), In(4)–Se(9) 258.30(14).

charge of the cluster anion. In the difference Fourier map, we found additional electron density on four symmetry-equivalent sites of the cluster, which were initially refined as one fourfold degenerated copper atom Cu(3). Compared to the cluster anion of **1**, this results in a reduction of the overall charge of the cluster anion from -2 to -1 if we assign the metal atoms as In^{3+} and Cu^+ . In agreement with this, we found only one tetraphenylarsonium counteranion in the crystal structure. However, the observed density could also be the result of four real atoms of roughly a quarter of the atomic number and weight (e.g. oxygen). In order to maintain the overall charge of the cluster at -1 , the electronic structure of the cluster must be significantly altered. Mass spectrometry and DFT computations were performed to address this problem (see further below). The additional copper atom [Cu(3)] is located in the middle of a six-membered ring [Se(4), In(1), Se(2), Cu(1'), Se(5'') and Cu(1'')] and has a nearly trigonal-planar coordination environment [Se–Cu–Se: 118.62(18) to 120.8(2)°]. The other copper atoms [Cu(1), Cu(2) and symmetry-equivalent positions] and indium atoms [In(1) and symmetry-equivalent positions] are all coordinated in distorted tetrahedral form by the selenium atoms of the SePh ligand [bond angles: Se–

Cu–Se 98.92(6)–123.55(5)°; Se–In–Se 103.23(3)–110.72(3)°]. As a consequence of the incorporation of an additional copper atom, the selenium atoms of the SePh ligands display a different set of bridging modes in **2** compared to those in **1**. Se(1), Se(1'), Se(1'') and Se(1''') are terminally bonded to In(1) and its symmetry-equivalent positions. Eight SePh ligands [Se(2), Se(2'), Se(2''), Se(2'''), Se(4), Se(4'), Se(4'') and Se(4''')] are μ_3 -bridging between two copper and one indium atom, whereas Se(3), Se(3'), Se(3'') and Se(3''') act as μ_2 bridges between two copper atoms. Se(5), Se(5'), Se(5'') and Se(5''') function as μ_4 bridges between four copper atoms. The Cu–SePh bond lengths range from 241.99(12) (Cu1–Se5) to 263.8(5) pm (Cu3–Se2) and the In–SePh bond lengths vary from 253.46(10) (In1–Se1) to 260.32(10) pm (In1–Se2).

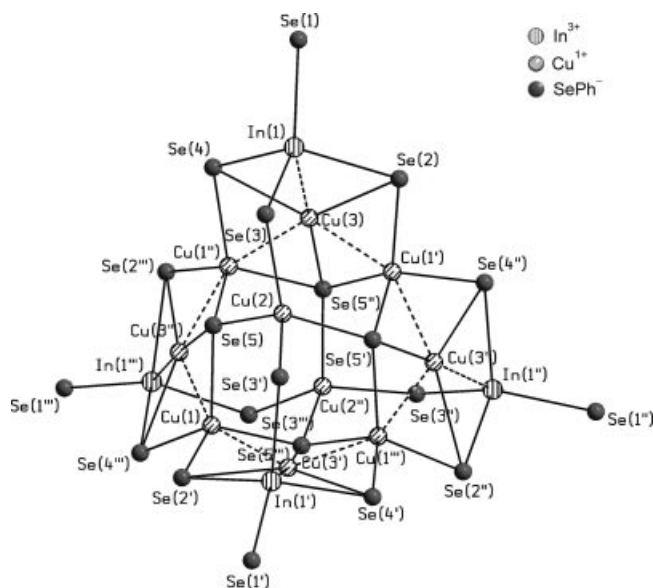


Figure 2. Molecular structure of the cluster anion $[\text{Cu}_7\text{In}_4(\text{SePh})_{20}]^-$ in $(\text{AsPh}_4)[\text{Cu}_7\text{In}_4(\text{SePh})_{20}]$ (**2**). C and H atoms are omitted for clarity. Selected bond length [pm] (solid lines): In(1)–Se(1) 253.46(10), In(1)–Se(3) 259.29(10), In(1)–Se(4) 260.25(9), In(1)–Se(2) 260.32(10), Cu(1)–Se(5) 241.99(12), Cu(1)–Se(5'') 243.92(12), Cu(1)–Se(2') 246.77(14), Cu(1)–Se(4'') 250.26(14), Cu(2)–Se(5) 245.96(12), Cu(2)–Se(5') 245.96(12), Cu(2)–Se(3') 247.40(12), Cu(2)–Se(3) 247.40(12), Cu(3)–Se(5'') 235.3(5), Cu(3)–Se(4) 251.5(5), Cu(3)–Se(2) 263.8(5), Se(2)–Cu(1') 246.77(14), Se(4)–Cu(1'') 250.26(14), Se(5)–Cu(3'') 235.3(5), Se(5)–Cu(1'') 243.92(12). Weak contacts [pm] (dashed lines): Cu(1)–Cu(3') 227.4(6), Cu(1)–Cu(3'') 228.4(5), In(1)–Cu(3) 261.0(5). Symmetry transformations for the generation of equivalent atoms: ' : $-x, -y - 1, z$; '' : $-y - 0.5, x - 0.5, -z + 0.5$; ''' : $y + 0.5, -x - 0.5, -z + 0.5$.

Kanatidis et al. reported the structure of a closely related singly charged cluster anion, $[\text{Cu}_6\text{In}_3(\text{SEt})_{16}]^-$, in which one $[(\mu_2\text{-SEt})_3\text{InSEt}]^-$ cap, which is needed to form the ideal four-fused adamantoid structure of $[\text{Cu}_6\text{In}_4(\text{SEt})_{20}]^{2-}$, is missing.^[1] Apparently, the hypothetical species of $[\text{Cu}_6\text{In}_4(\text{ER})_{20}]^{2-}$ (E = S, Se) is unstable as the dianion.

The solid-state UV/Vis spectra of **1** and **2** (Figure 3, bottom part) are quite similar, with a first shoulder at 400 nm (3.1 eV) and a broad maximum at 310 nm (4.0 eV). In solu-

tion, one observes similar absorption features with the bands shifted to 370 nm (3.4 eV) and 265 nm (4.7 eV), respectively. As mass spectrometry indicates the existence of the intact cluster anions in solution, the shift between solid-state and solution spectra likely arises from inhomogeneities of the crystal-oil mull between the quartz plates, which has been observed for other samples.^[21]

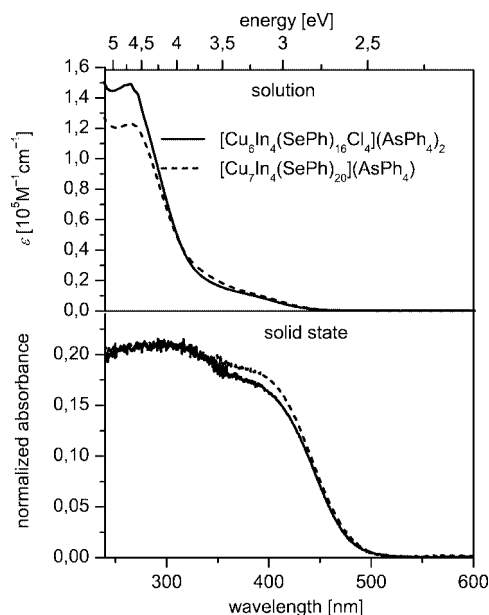


Figure 3. UV/Vis spectra of $(\text{AsPh}_4)_2[\text{Cu}_6\text{In}_4\text{Cl}_4(\text{SePh})_{16}]$ (**1**) and $(\text{AsPh}_4)[\text{Cu}_7\text{In}_4(\text{SePh})_{20}]$ (**2**) in solution (CH_2Cl_2) and in the solid state (mull in nujol between two quartz plates).

Mass Spectrometry

The additional charge density found in the X-ray diffraction analysis of compound **2**, leading to the proposed seventh (and fourfold degenerate) copper atom Cu(3), rendered another experimental technique desirable which might give further proof of the stoichiometry and charge state. Electrospray mass spectrometry, which has been proven very powerful for this class of compounds,^[22,23] was employed here in conjunction with collision-induced dissociation. The negative-ion mass spectrum of **2** (Figure 4) is governed by several strong ion signals which are all singly charged and can be clearly assigned as indicated in the graphic. The highest mass peak observed ($m/z \approx 4025$) is in complete agreement with the expected isotopomer distribution of the singly charged cluster anion $[\text{Cu}_7\text{In}_4(\text{SePh})_{20}]^-$, as can be seen from the inset in Figure 4. We note in passing that the two small peaks marked with an asterisk and shifted by 120 amu to lower mass are due to known ligand-exchange reactions of an SePh⁻ group with a Cl⁻ ion in solution, as has been observed previously.^[24,25] In order to answer the question whether the other strong ion signals next to the parent ion $[\text{Cu}_7\text{In}_4(\text{SePh})_{20}]^-$ could be explained as fragments of the gas-phase ion $[\text{Cu}_7\text{In}_4$ -

(SePh)₂₀][−], we performed a collision-induced dissociation study on the [Cu₇In₄(SePh)₂₀][−] cluster anion (Figure 5). Interestingly, the observed fragment ions differ significantly from the ion signals obtained by direct spraying of **2**. The fragmentation pattern indicates that the parent ion [Cu₇In₄(SePh)₂₀][−] first loses sequentially two In(SePh)₃ units from the corner sites of the tetrahedral cluster cage (see Figure 2) with further dissociation of Cu(SePh) units. On the other hand, the four major ion peaks of Figure 4 can be formally added up pairwise {namely [Cu₆In₃(SePh)₁₉][−]/[In(SePh)₄][−] and [Cu₃In₃(SePh)₁₃][−]/[Cu₃In(SePh)₇][−]} to give a [Cu₆In₄−

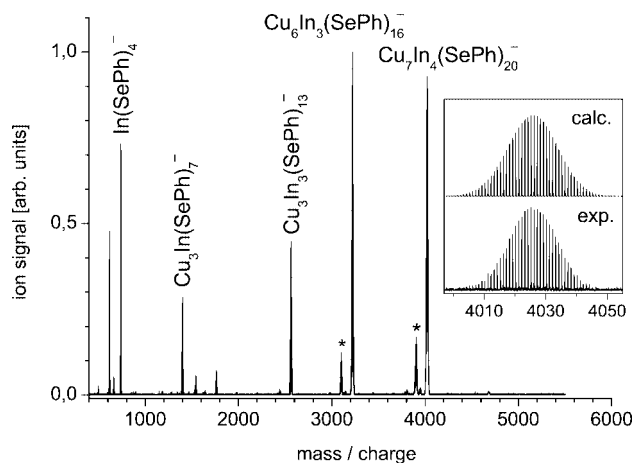


Figure 4. Negative-ion electrospray mass spectrum of **2**. The inset shows a high-resolution mass spectrum of the ion peak at $m/z \approx 4025$ displaying the isotopomer splitting in comparison to the calculated distribution expected for [Cu₇In₄(SePh)₂₀][−].

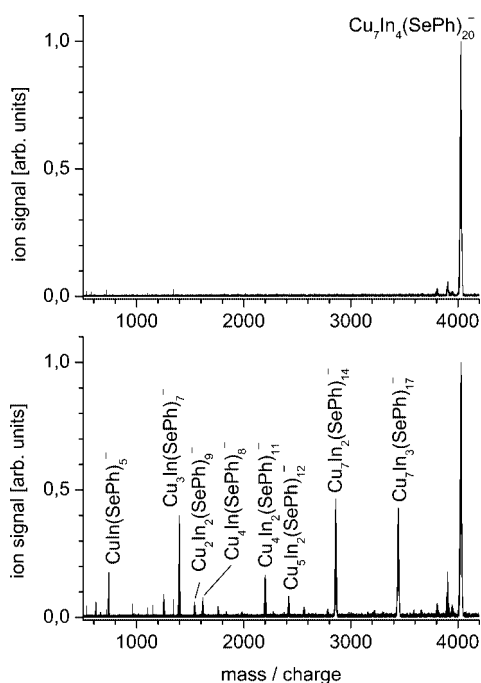


Figure 5. Mass spectrum of [Cu₇In₄(SePh)₂₀][−] isolated in the ICR cell (top panel) and after collision-induced dissociation with argon (bottom panel). The fragmentation pattern can be fully described by sequential loss of In(SePh)₃ and Cu(SePh) units consistent with the structure shown in Figure 2.

(SePh)₂₀]^{2−} entity which would rather point towards a solution-phase dissociation of **2**, i.e., loss of Cu⁺.

However, the fragmentation pattern of **2** strongly supports the identity of the parent ion as [Cu₇In₄(SePh)₂₀][−] ruling out other possibilities like the incorporation of oxygen.

DFT Calculations

For the Cu₇ compound, the X-ray structure has some ambiguities in assignment. The crystallographically imposed $\bar{4}$ symmetry distributes the effective electron density of the seventh copper atom over four identical sites, but the observed density could conceivably be due to four full-occupancy oxygen atoms. There should be, however, significant structural differences between the postulated Cu₇ and Cu₆O₄ cluster cores due to the vastly different electronic structure needed to maintain the −1 overall cluster charge.

Density functional theory has been successfully applied to similar cluster compounds,^[26] and should allow us to differentiate between these two putative assignments, as well as confirming that either are physically reasonable. The Cu₆O₄ case was quickly eliminated as it was highly unstable to geometry optimization and the electronic structure indicated a highly paramagnetic system, with essentially no HOMO–LUMO gap, contradicting the observed pale yellow color of the compound. The Cu₇ system was not, however, obviously the correct assignment. If addition of the seventh copper atom altered the rest of the cluster significantly from S_4 symmetry, the compound would be strongly disfavored from crystallizing in the observed space group.

Initial geometry optimization of the [Cu₇In₄(SeR)₂₀][−] anion was simplified by replacing the phenyl rings of the selenium ligands with methyl groups.^[27] Addition of a Cu⁺ ion to one of the adamantoid faces caused strong deviations in the geometry, the seventh copper atom having burrowed into the cluster, resulting in a related structure with C_2 symmetry. Geometry optimization of the fully phenylselenolate-ligated cluster proceeded successfully, with the extra copper atom remaining in the center of an external adamantoid face, and no major (e.g. bond-breaking) changes when compared to the crystal structure.

To test the assumption that the observed crystal structure is indeed the superposition of four orientations of [Cu₇In₄(SePh)₂₀][−], the DFT structure must be symmetrized under S_4 before comparison to experiment. The symmetrization procedure produced an averaged structure almost identical to that from the crystal, with an RMS distance of 13.7 pm between corresponding atoms in the superimposed structures, and well within the expected thermal motion. Calculated bonds in the cluster core tend to be consistently slightly longer than their respective distances in the crystal {calc – obs [pm]: In–Se: 4.30 ± 1.59 ; Cu–Se: 4.93 ± 2.01 ; Cu“7”–(Cu,Se): 5.15 ± 4.35 }, as is expected when comparing gas-phase to solid-state structures. The final electronic structure (diamagnetic, HOMO–LUMO gap = 1.7 eV) is also in agreement with observations.

Experimental Section

General: All experiments were carried out under dry nitrogen. CH_2Cl_2 and CH_3CN were dried with CaH_2 , followed by distillation under nitrogen. Anhydrous InCl_3 and Ph_4AsCl hydrate were obtained from Aldrich. $\text{Se}(\text{SiMe}_3)_2$ was prepared as reported in the literature.^[28] CuCl was subsequently washed with HCl , CH_3OH , and diethyl ether to remove traces of CuCl_2 , and dried under vacuum. $\text{Ph}_4\text{AsCl} \cdot x\text{H}_2\text{O}$ was dissolved in CH_3CN , dried with molecular sieves, and obtained as a white solid after filtration and removal of the solvent.

(AsPh_4)₂[$\text{Cu}_6\text{In}_4\text{Cl}_4(\text{SePh})_{16}$] (1): CuCl (55 mg, 0.56 mmol), InCl_3 (82 mg, 0.37 mmol), and Ph_4AsCl (78 mg, 0.19 mmol) were dissolved in CH_2Cl_2 (50 mL). After the solution was cooled to -20°C , PhSeSiMe_3 (0.47 mL, 1.9 mmol) was added. The final mixture was warmed to room temperature whilst stirring to give a yellow solution. Careful evaporation of the solvent yielded **1** as yellow crystalline needles. Yield: 263 mg; 67%. $\text{C}_{144}\text{H}_{120}\text{Cl}_4\text{Cu}_6\text{In}_4\text{Se}_{16}\text{As}_2$ (4246.1): calcd. C 40.73, H 2.85; found C 40.93, H 2.92.

(AsPh_4)₂[$\text{Cu}_7\text{In}_4(\text{SePh})_{20}$] (2): CuCl (43 mg, 0.43 mmol), InCl_3 (63 mg, 0.29 mmol), and Ph_4AsCl (60 mg, 0.14 mmol) were dissolved in CH_2Cl_2 (75 mL) and cooled to -20°C . PhSeSiMe_3 (0.52 mL, 2.15 mmol) was added to give a clear, orange solution. After stirring at room temperature for 24 h, the volume was reduced to 15 mL and left to stand. A few days later, orange blocks of **2** started to crystallize. Yield: 117 mg; 43%. $\text{C}_{144}\text{H}_{120}\text{Cu}_7\text{In}_4\text{Se}_{20}\text{As}$ (4408.8): calcd. C 39.23, H 2.74; found C 38.23, H 2.73.

Crystallography: Crystals suitable for single-crystal X-ray diffraction were taken directly from the reaction solution of the compound and then selected in perfluoroalkylether oil. Single-crystal X-ray diffraction data of **1** and **2** were collected using graphite-monochromatized Mo- K_α radiation ($\lambda = 0.71073 \text{ \AA}$) with a STOE IPDS II (Imaging Plate Diffraction System) equipped with a Schneider rotating anode. The structures were solved with the direct-methods program SHELXS^[29] of the SHELXTL PC suite of programs, and were refined with the use of the full-matrix least-squares program SHELXL.^[29] Molecular diagrams were prepared using SCHAKAL 97.^[30] All Cu, In, Se, As, Cl, and C atoms of the cluster molecules were refined with anisotropic displacement parameters, while Cl and C atoms of the solvent molecules were refined isotropically. CCDC-281603 (**1**) and -281604 (**2**) contain the supplementary crystallographic data for this paper. These data can be obtained free of charge from The Cambridge Crystallographic Data Centre via www.ccdc.cam.ac.uk/data_request/cif. X-ray powder diffraction patterns (XRD) were measured with a STOE STADI P diffractometer ($\text{Cu-K}_{\alpha 1}$ radiation, germanium monochromator, Debye–Scherrer geometry) in sealed glass capillaries. Simulated powder diffraction patterns for **1** and **2** were calculated on the basis of the atom coordinates obtained from single-crystal X-ray analysis by using the program package STOE WinXPOW.^[31]

Mass Spectrometry: Mass spectrometry was performed with a 7T-Fourier transform ion cyclotron resonance (FT-ICR) mass spectrometer (Bruker Daltonics, Billerica, MA, USA), equipped with an electrospray ionization source (Analytica of Branford, Branford, CT, USA) which has been modified by us for improved ion sensitivity by means of home-built ion optics. Solutions of **1** and **2** in CH_2Cl_2 were prepared at a concentration of ca. 0.1 mmol/L under nitrogen and sprayed at typical flow rates of 300 $\mu\text{L/h}$. Collision-induced dissociation experiments were taken in an MS/MS mode, i.e., the parent ion of interest was first mass-selected in the ICR cell by standard ICR techniques (resonant ejection sweeps) and subjected to collisions with argon ($p = 5 \cdot 10^{-8} \text{ mbar}$) at elevated kinetic energies to induce fragmentation.

Physical Measurements: UV/Vis absorption spectra of cluster molecules in solution were measured with a Varian Cary 500 spectrophotometer in quartz cuvettes. Solid-state reflection spectra were measured as micron-sized crystalline powders between quartz plates with a Labsphere integrating sphere.

Calculation Technical Details: Density functional theory calculations were performed with the TURBOMOLE program package^[32] employing the BP86 functional with the very efficient MARI-J approximation,^[33] and TZVP basis set.^[34] Starting geometries were adapted from the crystal structure, and then optimized with default convergence criteria. Due to electronic convergence problems, the $[\text{Cu}_6\text{O}_4\text{In}_4(\text{SePh})_{20}]^-$ cluster was calculated spin-unrestricted with Fermi electronic occupation smearing. The metal–chalcogen core of the seven-copper cluster was symmetrized while ignoring the seventh copper atom. The pseudo- S_4 axis was determined by a simple linear combination of symmetry-related (in the ideal case) atom position vectors, and was then re-oriented to bring the axis in line with $+z$. The symmetry-equivalent coordinates were averaged, and the cluster was rotated about the z axis to minimize differences with the X-ray data.

Acknowledgments

This work was supported by the Deutsche Forschungsgemeinschaft (Center for Functional Nanostructures CFN).

- [1] W. Hirpo, S. Dhingra, M. Kanatzidis, *Chem. Commun.* **1992**, 557–559.
- [2] J. Olkowska-Oetzel, D. Fenske, P. Scheer, A. Eichhöfer, *Z. Anorg. Allg. Chem.* **2003**, 629, 415–420.
- [3] A. Eichhöfer, D. Fenske, *J. Chem. Soc., Dalton Trans.* **2000**, 941–944.
- [4] R. Ahlrichs, A. Eichhöfer, D. Fenske, O. Hampe, M. M. Kappes, P. Nava, J. Olkowska-Oetzel, *Angew. Chem.* **2004**, 116, 3911–3915; *Angew. Chem. Int. Ed.* **2004**, 43, 3823–3827.
- [5] D. T. T. Tran, L. M. C. Beltran, C. M. Kowalchuk, N. R. Trefiak, N. J. Taylor, J. F. Corrigan, *Inorg. Chem.* **2002**, 41, 5693–5698.
- [6] D. T. T. Tran, N. J. Taylor, J. F. Corrigan, *Angew. Chem.* **2000**, 112, 965–967; *Angew. Chem. Int. Ed.* **2000**, 39, 935–937.
- [7] A. Lorenz, D. Fenske, *Angew. Chem.* **2001**, 113, 4537–4541; *Angew. Chem. Int. Ed.* **2001**, 40, 4402; A. Lorenz, D. Fenske, *Z. Anorg. Allg. Chem.* **2001**, 627, 2232–2248.
- [8] R. Pätow, D. Fenske, *Z. Anorg. Allg. Chem.* **2002**, 628, 1279–1288.
- [9] M. W. DeGroot, N. J. Taylor, J. F. Corrigan, *J. Am. Chem. Soc.* **2003**, 125, 864–865.
- [10] W. Hirpo, S. Dhingra, A. C. Sutorik, M. Kanatzidis, *J. Am. Chem. Soc.* **1993**, 115, 1597–1599.
- [11] P. Strickler, *J. Chem. Soc. D* **1969**, 655b–656.
- [12] A. Choy, D. Craig, I. G. Dance, M. L. Scudder, *J. Chem. Soc., Chem. Commun.* **1982**, 1246–1247.
- [13] I. G. Dance, A. Choy, M. L. Scudder, *J. Am. Chem. Soc.* **1984**, 106, 6285–6295.
- [14] S. Behrens, M. Bettenhausen, A. Eichhöfer, D. Fenske, *Angew. Chem.* **1997**, 109, 2874–2876; S. Behrens, M. Bettenhausen, A. Eichhöfer, D. Fenske, *Angew. Chem. Int. Ed. Engl.* **1997**, 24, 2797.
- [15] A. Eichhöfer, D. Fenske, H. Pfistner, M. Wunder, *Z. Anorg. Allg. Chem.* **1998**, 624, 1909–1914.
- [16] A. Eichhöfer, A. Aharoni, U. Banin, *Z. Anorg. Allg. Chem.* **2002**, 628, 2415–2421.
- [17] A. Eichhöfer, E. Tröster, *Eur. J. Inorg. Chem.* **2002**, 2253–2256.
- [18] A. Eichhöfer, P. Deglmann, *Eur. J. Inorg. Chem.* **2004**, 349–355.
- [19] M. W. DeGroot, J. F. Corrigan, *Angew. Chem.* **2004**, 116, 5469–5471; *Angew. Chem. Int. Ed.* **2004**, 43, 5355–5357.

- [20] Ch. Wang, X. Bu, N. Zheng, P. Feng, *Chem. Commun.* **2002**, 1344–1345.
- [21] A. Eichhöfer, O. Hampe, M. Blom, *Eur. J. Inorg. Chem.* **2003**, 1307–1314.
- [22] A. Eichhöfer, O. Hampe, *Chem. Phys. Lett.* **2005**, 407, 186–191.
- [23] D. Fenske, T. Langetepe, M. Kappes, O. Hampe, P. Weis, *Angew. Chem.* **2000**, 112, 1925–1928; *Angew. Chem. Int. Ed.* **2000**, 39, 1857–1860.
- [24] T. Løver, W. Henderson, G. A. Bowmaker, J. M. Seakins, R. P. Cooney, *Inorg. Chem.* **1997**, 36, 3711–3723.
- [25] J.-J. Gaumet, G. F. Strouse, *J. Am. Soc. Mass Spectrom.* **2000**, 11, 338–344.
- [26] R. Ahlrichs, D. Fenske, M. McPartlin, A. Rothenberger, C. Schroth, S. Wieber, *Angew. Chem.* **2005**, 117, 4002–4005; *Angew. Chem. Int. Ed.* **2005**, 44, 3932–3936.
- [27] A test optimization of the related $[\text{Cu}_6]^{2-}$ cluster converged to a geometry very close to that of the anion in the crystal structure of Cu_7 .
- [28] G. Brauer (Ed.), *Handbuch der Präparativen Anorganischen Chemie*, 3rd ed., Enke-Verlag, Stuttgart, **1975**, vol. 1, p. 372.
- [29] G. M. Sheldrick, *SHELXTL PC version 5.1, An Integrated System for Solving, Refining, and Displaying Crystal Structures from Diffraction Data*, Bruker Analytical X-ray Systems, Karlsruhe, **2000**.
- [30] E. Keller, *SCHAKAL 97, A Computer Program for the Graphic Representation of Molecular and Crystallographic Models*, University of Freiburg, **1997**.
- [31] STOE, *WinXPOW*, STOE & Cie GmbH, Darmstadt, **2000**.
- [32] R. Ahlrichs, M. Bär, M. Häser, H. Horn, C. Kölmel, *Chem. Phys. Lett.* **1989**, 162, 165–169; O. Treutler, R. Ahlrichs, *J. Chem. Phys.* **1995**, 102, 346–354.
- [33] A. D. Becke, *Phys. Rev. A* **1988**, 38, 3098–3100; S. J. Vosko, L. Wilk, M. Nusair, *Can. J. Phys.* **1980**, 58, 1200–1211; J. P. Perdew, *Phys. Rev. B* **1986**, 33, 8822–8824; erratum; J. P. Perdew, *Phys. Rev. B* **1986**, 34, 7406; K. Eichkorn, O. Treutler, H. Öhm, M. Häser, R. Ahlrichs, *Chem. Phys. Lett.* **1995**, 242, 652–660; M. Sierka, A. Hogekamp, R. Ahlrichs, *J. Chem. Phys.* **2003**, 118, 9136–9148.
- [34] Available at <ftp://ftp.chemie.uni-karlsruhe.de/pub/>.

Received: September 14, 2005

Published Online: December 1, 2005